Journal of Electrical Engineering and Renewable Energies Development (JEERED)
Issue N°: 1, Vol. N°: 1, pp. 33-40, 2025

Fuzzy Logic Control for Enhanced 4WD Electric Vehicle Speed Control

ABDELHAMID Bouregba [1], AISSA Benhammou[1], ABDELDJABAR Hazzab[2], SAMIR Hadjeri[3]

(1) SGRE laboratory,Tahri Mohamed University Bechar, Algeria

(2) University of Quebec, Canada

(3) University of Sidi Bel Abbes, Algeria

Email of corresponding author: Benhammou.aissa@univ-bechar.dz

Abstract—This study explains the implementation and design of a Fuzzy Logic Controller (FLC) for enhanced speed control in a four-wheel-drive (4WD) electric vehicle (EV). Traditional Proportional-Integral-Derivative (PID) controllers often struggle with the nonlinear dynamics, parameter variations, and external disturbances inherent in EV systems. To address these challenges, we propose an intelligent FLC that leverages heuristic knowledge to provide robust and adaptive control without requiring a precise mathematical model. The controller's performance is evaluated through simulation under various driving conditions, including different road surfaces and sudden load changes. Results demonstrate that the proposed FLC system achieves superior performance compared to a conventional PI controller, exhibiting significantly reduced rise and settling times, minimal overshoot, and enhanced stability, thereby ensuring improved traction, energy efficiency, and driving comfort.

Keywords— *Electric vehicle, 4 wheel-drive, induction motor, Fuzzy Logic control, Exponential reaching law.*

I. INTRODUCTION

Recently, the automotive industry has known a significant interest in the adoption of electric drives for vehicle traction, for reasons of sustainability, emissions reductions, and energy efficiency[1]. This shift has spurred the large-scale emergence of different categories of electric vehicles, such as battery-powered models, hybrid electric vehicles, and fuel cell electric vehicles. As a result, drivetrain technologies have become a focal point of research and innovation, with a strong emphasis on improving efficiency, performance, and reliability for the foreseeable future. A vehicle's driving performance is typically assessed based on key metrics such as acceleration time, maximum velocity, and road gradeability. At the heart of the electric propulsion system lies the electrical motor, which serves as its essential component. Recently, leading international vehicle manufacturers have increasingly employed induction motors (IMs) and permanent magnet motors (PMs) in their electric vehicle designs due to their high efficiency, reliability, and adaptability[2].

According to industry evaluations and surveys conducted among electric vehicle commercial companies, the IM has emerged as a preferred choice for EV drivetrain systems (EVDS) due to its robustness, lower cost, and ability to operate effectively under a wide range of conditions. Control of speed in electric vehicles (EVs) is crucial for enhancing the performance, efficiency, and general functionality of EV traction systems. As an important part of the electric powertrain, speed regulation lets the car adapt to different driving conditions, such as sudden acceleration, deceleration, or changes in road gradient, while still keeping smooth and precise control over how the motor operate[3].

In fact, the IM presents a high coupling between flux and torque. making the control of induction motors more challenging, as adjustments to one parameter inevitably influence the other. To address this complexity, the researchers have developed many control propositions, such as classical scalar control, and classical vector control, or field-oriented control. The scalar control technique is widely recognized for its simple structure and ease of

implementation, making it an attractive solution and can provide acceptable steady-state performances for IM drive control. However, the limitations of scalar control become apparent during transient conditions, such as sudden changes in load or speed. Vector control allows for accurate and smooth control of both flux and torque, even during rapid changes in operating conditions. However, this technique has a high sensitivity to the machine parameters variations and requires a precise mathematical model of the IM, accurate measurement, and sophisticated control method, increasing the complexity in term of hardware requirements, computational resources, and implementation[4].

The proposition of adaptative neural fuzzy inference system (ANFIS) by Benhammou and all in [2] has resulted some ripples in the law speed test due to the requirement adaptation of the controllers.

However, the design of traditional controllers like PID often struggles with the nonlinear dynamics, parameter variations, and external disturbances inherent in electric vehicle systems. To overcome these limitations, intelligent control strategies have been developed to provide robust performance without requiring a precise mathematical model. One such method is Fuzzy Logic Control (FLC), which uses heuristic knowledge and a rule-based system to manage system complexities. This approach maintains the system's stability and robustness while offering inherently smooth control action, effectively avoiding the chattering phenomenon altogether. The main goal of this study is to investigate a Fuzzy Logic Controller for 4WDEV speed control. In the outer speed control loop, an FLC was designed to deliver high control performance, ensure system stability and robustness, and enhance the dynamic behavior of the EV [3].

Analysis of recent research. In [8], a hybrid fuzzy sliding mode controller was developed... [9-17] can remain mostly unchanged as they provide context on hybrid and intelligent methods, though the concluding "Motivated by" section should be adjusted].

Motivated by the advantages of the above studies, in this research, a fuzzy logic controller is used to directly determine the optimal control effort based on the error in speed and its rate of change. The FLC's rule-based system is designed to provide an adaptive and robust response to variations in operating conditions and external load disturbances. This study represents a valuable solution that inherently avoids the problems induced by the chattering phenomenon and allows the controller to achieve a smooth control signal. In general, the main objectives of this study can be summarized as follows:

A mathematical design procedure of a speed controller based on indirect FOC for a 4WDEV.

The design of a Fuzzy Logic Controller to replace traditional methods, eliminating the challenge of chattering.

The fuzzy logic system is designed based on the transient and steady-state conditions of the control system states to ensure robust performance.

II. MODELLING OF EV DRIVING

Effective speed control in accordance with a predefined driving cycle requires a comprehensive vehicle model. This model uses the target velocity from the driving cycle as input, while the control system interfaces directly with the inverter. The inverter plays a crucial role by converting the electrical energy from the battery into a suitable form specifically, a reference rotational speed and load torque for the IM. The IM then converts this electrical energy into mechanical power, which ultimately propels the vehicle. Figure (1) provides a visual representation of the various components that constitute the EV propulsion system, highlighting the seamless integration of these elements to achieve efficient and responsive vehicle performance [18].

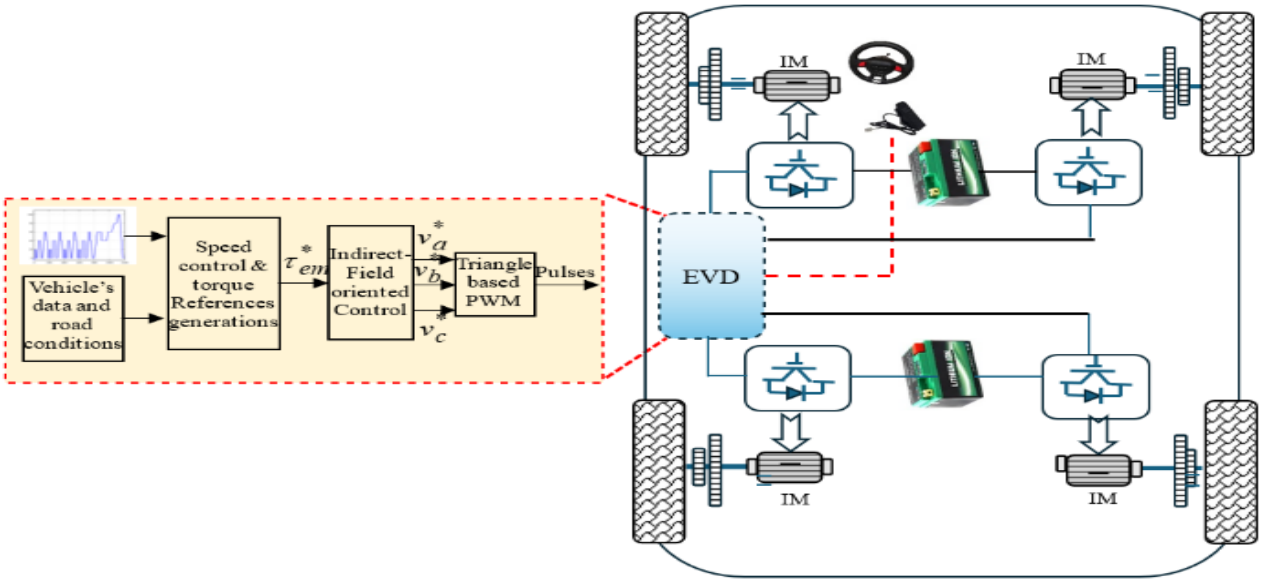

Fig. 1. The various components that constitute the EV propulsion system.

II.1. EV DYNAMIC MODEL

Utilizing a dynamic model plays a crucial role in enhancing the overall efficiency of EVs, as it allows for the optimization of propulsion system design, and the evaluation of vehicle performance under realistic conditions. Consider an EV with mass Mv moving at speed V along a path inclined at an angle δ to the horizontal. A dynamic model can be formulated by representing the vehicle as a rigid body subjected to various resistance forces acting along the longitudinal axis. These include: aerodynamic drag, resulting from the relative motion between the vehicle and ambient air; rolling resistance, caused by friction between the tires and the road surface; grade resistance, associated with the slope of the road; and inertial (or acceleration) resistance, representing the force required to change the vehicle's velocity. Together, these resistive forces define the total tractive effort required to propel the vehicle and have a direct impact on energy consumption and control strategy effectiveness, as illustrated in Figure (2) [8].

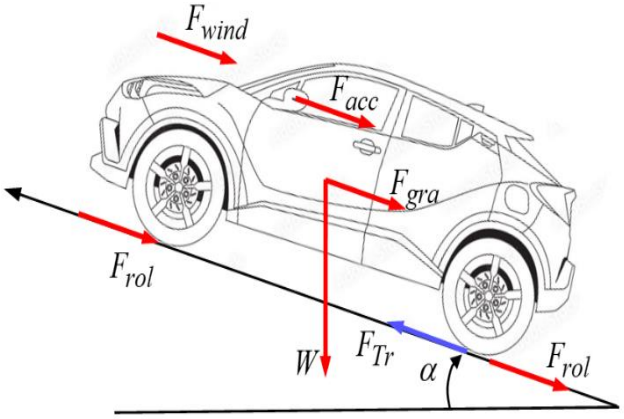

Fig. 2. Forces exerted on the four-wheel drive electric vehicle.

After the application of the second law of Newton, the obtained expression formulated as follows:

$$M_v \frac{d\vec{v}}{dt} = \sum \vec{F}_{ext} = \vec{F}_{Tr} + \vec{F}_{acc} + \vec{F}_{rol} + \vec{F}_{wind} + \vec{F}_{gra} \quad (1)$$

The projection of the law onto the horizontal axis leads to:

$$M_v \frac{dv}{dt} = \sum F_{ext} = F_{Tr_x} - \left(F_{acc_x} + F_{rol_x} + F_{wind_x} + F_{gra_x}\right) \quad (2)$$

Where:

$$F_{wind_x} = \frac{1}{2}\rho S C_x (v - v_0)^2 \quad (3)$$

$$F_{gra_x} = G_r M_v g \cos(\alpha) \quad (4)$$

$$W_x = M_v g \sin(\alpha) \quad (5)$$

$$F_{acc_x} = M_v \frac{dv}{dt} \quad (6)$$

Where F_{Tr} represents the total tractive force, F_{wind} the force of wind resistance, F_{rol} the force of rolling resistance, F_{gra} the force of grading resistance, F_{acc} the force of acceleration, and C_{win} , and C_{rol} symbolize the wind and rolling resistance coefficient, respectively, while m is the vehicle mass, and g is the gravitational force. The wheel radius, gear ratio, and vehicle velocity are represented by w_r, G_r, and V_V , respectively.

$$\omega_r = G_r \frac{V_v}{R_{wheel}}, \text{ and } \omega_{wheel} = \frac{V_v}{R_{wheel}} \quad (7)$$

The motor load torque T_L can be formulated as function of speed as follow:

$$T_L = \frac{1}{G_r} T_w = \frac{1}{G_r}\left(F_{wind} + F_{rol} + F_{acc} + F_{gra}\right) \quad (8)$$

II.2. MODELLING AND FIELD ORIENTED CONTROL OF AN INDUCTION MOTOR

The dynamic model of the three phase Y-connected induction motor can be written in the d-q synchronous frame by the following differential equations [19], [20];

$$\frac{di_{ds}}{dt} = \frac{1}{\sigma L_s}\left(-R_{eq} i_{ds} + \sigma L_s \omega_s i_{qs} + \frac{L_m R_r}{L_r^2}\varphi_{dr} + P\frac{L_m}{L_r}\varphi_{qr}\omega_r + v_{ds}\right) \quad (9)$$

$$\frac{di_{qs}}{dt} = \frac{1}{\sigma L_s}\left(-\sigma L_s \omega_s i_{ds} - R_{eq} i_{qs} - P\frac{L_m}{L_r}\varphi_{dr}\omega_r + \frac{L_m R_r}{L_r^2}\varphi_{qr} + v_{qs}\right) \quad (10)$$

$$\frac{d\varphi_{dr}}{dt} = \frac{L_m R_r}{L_r} i_{ds} - \frac{R_r}{L_r}\varphi_{dr} + (\omega_s - P\omega_r)\varphi_{qr} \quad (11)$$

$$\frac{d\varphi_{qr}}{dt} = \frac{L_m R_r}{L_r}.\, i_{qs} - (\omega_s - P\omega_r).\, \varphi_{dr} - \frac{R_r}{L_r}.\, \varphi_{qr} \quad (12)$$

$$\frac{d\omega_r}{dt} = \frac{1}{J}\left(\frac{3}{2}\frac{P.L_m}{L_r}.\left(i_{qs}.\varphi_{dr} - i_{ds}.\varphi_{qr}\right) - f_c.\omega_r - .T_l\right) \quad (13)$$

Where R_s, R_r denote the stator and rotor resistance per phase, L_m is the magnetizing inductance per phase.L_s , L_r are the stator inductance and rotor inductance per phase, ω_s denotes the synchronous frequency and ω_r is rotor frequency, P the number of pole pairs, $\tau_r = L_r/R_r$ the rotor time-constant, $\sigma = 1 - [L_m^2/(L_s L_r)]$ represents the leakage coefficient, i_{ds} and i_{qs} d-axis and q-axis stator current, φ_{dr} and φ_{qr} d-axis and q-axis rotor flux, v_{ds} and v_{qs} are d-axis and q-axis stator voltage,$R_{eq} = (R_s + (L_m/L_r)^2 R_r)$. And the electromagnetic torque can be written as given in (14):

$$T_e = \frac{3PL_m}{2L_r}\left(i_{qs}\varphi_{dr} - i_{ds}\varphi_{qr}\right) \quad (14)$$

The dynamic behavior of an induction motor under vector control is analogous to that of a separately excited DC machine, since torque and flux can be regulated independently. In the case of perfect rotor-flux orientation, the quadrature component of the rotor flux φ_{qr} is set to equal zero, then we can write as given in (15) and (16):

$$\varphi_{qr} = 0 \quad (15)$$

$$\varphi_{dr} = \varphi_r^N = \text{constant} \quad (16)$$

Where: φ_r^N denotes the rotor flux rated value

Consequently, the torque equation is simplified to become like a DC motor torque equation as follows

$$T_e = \frac{3PL_m}{2L_r} i_{qs} \varphi_{dr} \quad (17)$$

And the slip frequency, $\omega_{sl} = \omega_s - P\omega_r$, is computed by the following equation:

$$\omega_{sl} = \frac{1}{\tau_r} \frac{i_{qs}^*}{i_{ds}^*} \quad (18)$$

where superscript (*) represents reference values.

III. THE ELECTRONIC DIFFERENTIAL PRINCIPLE

The electronic differential system (EDS) used in four-wheel-independent electric vehicles is a sophisticated control architecture. In the proposed scheme (Fig. 3), each wheel front left, front right, rear left, and rear right is driven by its own in-wheel motor under independent control. Induction machines are selected as traction motors because they offer good efficiency, high torque density, low acoustic noise, and overall suitability for electric-vehicle traction[21-26].

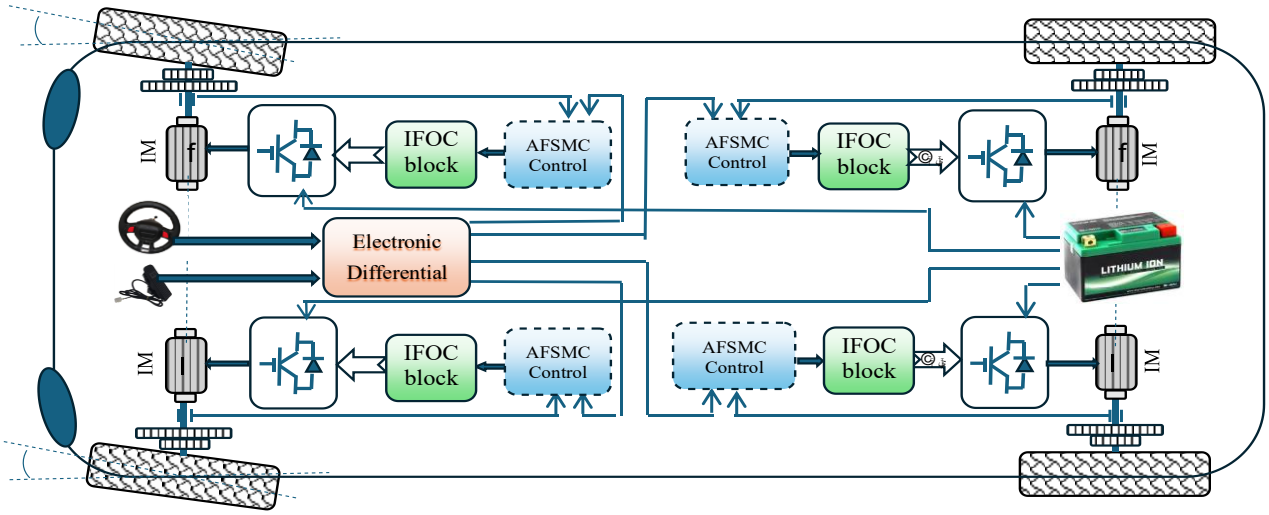

Fig. 3. The EV4WD under study

The reference speed for the four drive wheels is defined as follows:

$$\omega_{lr}^* = \omega_{veh} \frac{\sqrt{1+\left(cos(\delta)-\frac{d_\omega}{2L_\omega}\right)^2}}{\sqrt{1+(cos(\delta))^2}} \quad (32)$$

$$\omega_{rr}^* = \omega_{veh} \frac{\sqrt{1+\left(cos(\delta)+\frac{d_\omega}{2L_\omega}\right)^2}}{\sqrt{1+(cos(\delta))^2}} \quad (33)$$

$$\omega_{lf}^* = \omega_{veh} \left(1 - \frac{d_\omega tan(\delta)}{2L_\omega}\right) \quad (34)$$

$$\omega_{rf}^* = \omega_{veh} \left(1 + \frac{d_\omega tan(\delta)}{2L_\omega}\right) \quad (35)$$

Where: (*) indicates the reference parameter, ω_{lr} is the left rear wheel speed, $\omega_{rr}$is the right rear wheel speed, $\omega_{lf}$is the left front wheel speed, $\omega_{rf}$is the right front wheel speed, $\omega_{veh}$is the EV speed $d_\omega$and $L_\omega$are distance between left and right drive wheels and the distance between the front and rear axles.

IV. SIMULATION RESULTS

To thoroughly assess the performance of the proposed FLC control, a series of simulations encompassing two distinct test scenarios was carried out using the MATLAB/Simulink platform. These test cases were designed to evaluate the controller's effectiveness under various dynamic conditions. The vehicle parameters and system specifications employed in the simulations are detailed in Tables 1 and 2.

TABLE 1 NOMINAL IM PARAMETERS VALUES [8]

Parameter	*Value*
Rated Power P_n	*37 Kw*
Line-Line voltage V_n	*400 V*
Rated current I_n	*64 A*
Rated Speed ω_n	*2960 rpm*
.Number of pole pairs *P*	*1*
Stator resistance R_s	*85.1 mΩ*
Rotor resistance R_r	*65.8 mΩ*
Stator Inductance L_s	*31.4 Mh*
Rotor Inductance L_r	*31.4 Mh*
Magnetizing Inductance L_m	*29.1 mH*
Inertia Moment of motor *j*	*0.23 kg/m2*
Friction coefficient f_c	*0.0095Nm.s/rad*

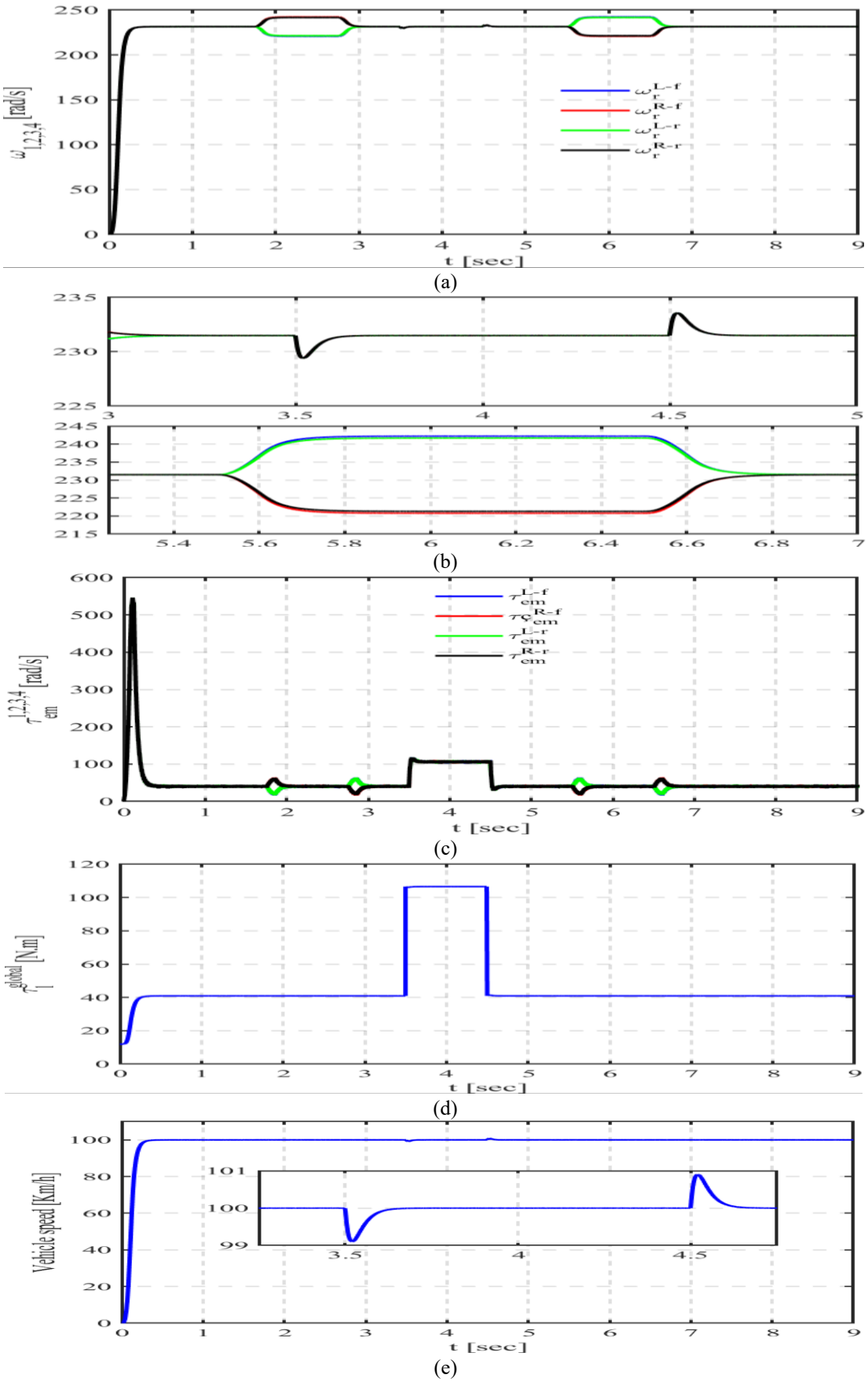

Fig.4: EV behaviour, (a) EV wheels speed [rpm]; (b) ZOOM of speed;(c) Wheels ‘s electromagnetic torque [N.m]; (d) Load torque (Nm); and (e) EV speed.

TABLE 2 EV MECHANICAL AND AERODYNAMIC PARAMETERS [8]

Parameter	*Value*
m	*150 kg*
A	*1.8 m^2*
R	*0.3 m*
μ_{rr1}	*0.0055*
μ_{rr2}	*0.056*
Cad	*0.19*
G	*104*
η_g	*0.95*
T	*57.2 Nm*
v_0	*4.155 m/s*
g	*9.81 m/s^2*
ρ	*0.23 kg/m^3*

A. CASE 01

To validate the FLC technique on the 4WDEV traction system, the system was subjected to a variation in the reference speed while incorporating realistic driving maneuvers. At this test stage, the driver commands two distinct turns using the steering angle input.

The first maneuver (Phase 01), a left turn, occurs at t = 8 s, followed by a right turn at t = 28 s. Figure (4) displays the linear velocity of each wheel during the turning sequences at constant speed. The driver-defined reference angle δ is applied initially to the front wheels.

In response, the EDS dynamically adjusts the individual speeds of all four induction motors. During the right turn, the EDS reduces the speed of the inner wheels (right side) while increasing that of the outer wheels (left side), ensuring optimal torque distribution and turning stability. Specifically, in Phase 01, the front-left and rear-left wheels rotate faster than their right-side counterparts, highlighting the adaptive behavior of the control system. A similar pattern is observed during the second phase with the appropriate inversion of speed roles. Figue (4-a) clearly demonstrates the speed differentiation among the four wheels during cornering, confirming the precise and real-time intervention of the FLC-EDS strategy.

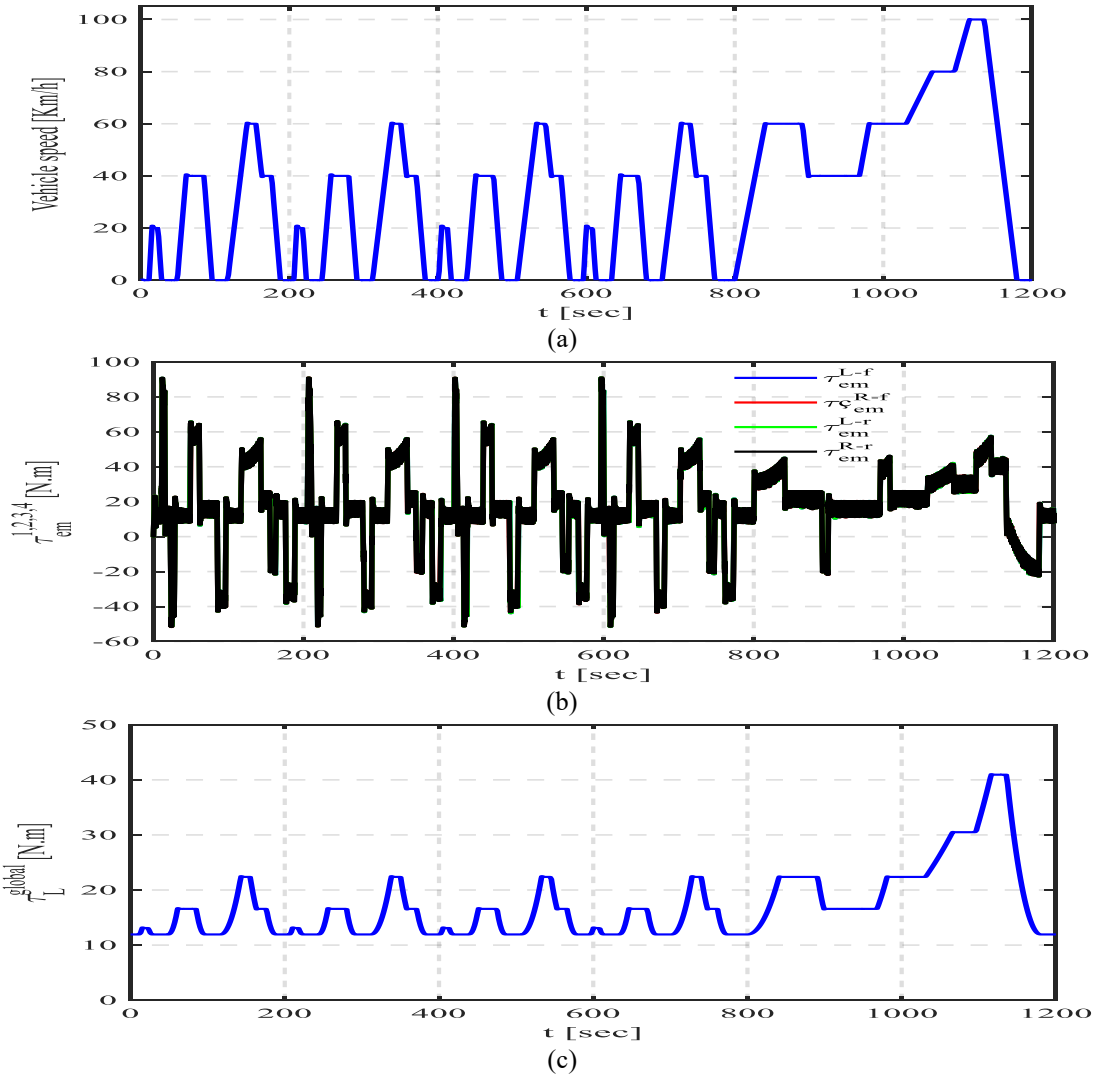

Fig.5. EV scenario, (a) European Driving Cycle (EDC) Speed Profile Applied to the 4WD Electric Vehicle; (b) Electromagnetic Torque Response Under the Proposed Control Strategy; (c)Load Torque Variation Corresponding to Realistic Driving Conditions.

B. Case 02

In this study, the dynamic response of the EV propulsion system is implemented and evaluated under the standardized New European Driving Cycle (NEDC), which includes both urban (ECE-15) and extra-urban (EUDC) driving phases, offering a comprehensive scenario for assessing energy consumption, motor performance, and system efficiency. During the simulation, the focus is placed on analyzing the current drawn by the electric motor from the power supply across all operational modes of the cycle. These include acceleration phases, where high torque demands significantly increase current consumption; cruising phases, where maintaining steady-state efficiency and minimizing current fluctuations are essential; and deceleration or regenerative braking phases, where the energy recovery potential is critically assessed. Through detailed examination of the current profiles, key insights are obtained regarding motor efficiency, power electronic losses, and total energy consumption. This analysis further identifies opportunities to optimize control strategies such as FOC to reduce energy losses and extend battery life. In addition, the simulated current waveforms are compared with ideal theoretical models to detect deviations caused by nonlinear motor characteristics, switching harmonics, and load variations. These results provide a deeper understanding of real-world energy usage and validate the proposed fuzzy logic control strategy's effectiveness in minimizing peak current demand while maintaining robust driving performance throughout the NEDC.

Figure (5) illustrates the EV scenario over a duration of 1200 seconds, where Figure (5-a) shows the EV speed profile, Figure (5-b) presents the electromagnetic torque for each wheel, and Fig.5(c) depicts the variation of load torque under realistic driving conditions.

As highlighted from simulations results, the proposed approach outperforms the reference method across several critical aspects. Unlike the conventional PI strategies, which offer limited robustness and are susceptible to performance degradation under varying conditions, the FLC integrates an intelligent computing mechanism to improve the control system responses. This significantly enhances system robustness and tracking accuracy. Moreover, the proposed strategy demonstrates superior adaptability to complex driving scenarios, including slope variation, curved paths, and the NEDC standard cycle, while maintaining better energy efficiency and motor current regulation. Overall, the current study clearly emphasizes the practical and theoretical advantages of the FLC approach, making it a promising candidate for advanced EV motion control systems.

V. CONCLUSIONS.

In this paper, a novel FLC control has been presented to enhance the speed tracking performance of a 4WD-EV. The developed control strategy demonstrates superior stability across diverse driving scenarios, including sharp turns and uneven slopes, while contributing to improved energy efficiency. By effectively minimizing torque and flux ripples particularly during startup phases the controller significantly reduces energy losses and extends the vehicle's driving range, which is critical in electric vehicles where energy optimization directly affects driving autonomy.

The effectiveness of the proposed FLC structure was verified through high-fidelity simulations in MATLAB/Simulink, benchmarking its performance against that of the conventional PI. The simulation results reveal a faster dynamic response in torque and flux, and improved speed tracking accuracy. Moreover, the fuzzy logic controller mechanism enhances robustness by effectively compensating for load variations and external disturbances, ensuring consistent performance under realistic driving conditions.

REFERENCES

[1] A. Kimouche, M. R. Mekideche, M. Chebout, and H. Allag, "Influence of permanent magnet parameters on the performances of claw pole machines used in hybrid vehicles," Electrical Engineering & Electromechanics, no. 4, Art. no. 4, Jun. 2024, pp. 3-8. doi: 10.20998/2074-272X.2024.4.01.

[2] Benhammou, H. Tedjini, Y. Guettaf, M.A. Soumeur, M.A. Hartani, O. Hafsi, A. Benabdelkader, "Exploitation of vehicle's kinetic energy in power management of tow -wheel drive electric vehicles based on ANFIS DTC-SVM comparative study," International Journal of Hydrogen Energy, vol. 46, no. 54, pp. 27758–27769, Aug. 2021, doi: 10.1016/j.ijhydene.2021.06.023.

[3] L. Djafer, R. Taleb, F. Mehedi, A. Aissa Bokhtache, T. Bessaad, F. Chabni, H. Saidi, "Electric drive vehicle based on sliding mode control technique using a 21-level asymmetrical inverter under different operating conditions," Electrical Engineering & Electromechanics, no. 3, May 2025, pp. 31-36 doi: 10.20998/2074-272X.2025.3.05.

[4] K. Abed and H. K. E. Zine, "Intelligent fuzzy back-stepping observer design based induction motor robust nonlinear sensorless control," Electrical Engineering & Electromechanics, no. 2,. Feb. 2024, pp. 10-15, doi: 10.20998/2074-272X.2024.2.02.

[5] O. Oualah, D. Kerdoun, and A. Boumassata, "Comparative study between sliding mode control and the vector control of a brushless doubly fed reluctance generator based on wind energy conversion systems," Electrical Engineering & Electromechanics,. no.1, Feb. 2022, pp. 51-58, doi: 10.20998/2074-272X.2022.1.07.

[6] O. Oualah, D. Kerdoun, and A. Boumassata, "Super-twisting sliding mode control for brushless doubly fed reluctance generator based on wind energy conversion system," Electrical Engineering & Electromechanics, no. 2, Mar. 2023, pp. 86-92. doi: 10.20998/2074-272X.2023.2.13.

[7] D. Sakri, H. Laib, S. E. Farhi, and N. Golea, "Sliding mode approach for control and observation of a three phase AC-DC pulse-width modulation rectifier," Electrical Engineering & Electromechanics, no. 2, Mar. 2023, pp.49-56. doi: 10.20998/2074-272X.2023.2.08.

[8] D. Cherifi and Y. Miloud, "Hybrid Control Using Adaptive Fuzzy Sliding Mode Control of Doubly Fed Induction Generator for Wind Energy Conversion System," Periodica Polytechnica Electrical Engineering and Computer Science, vol. 64, no. 4, Art. no. 4, Sep. 2020, doi: 10.3311/PPee.15508.

[9] F. F. M. El-Sousy, M. M. Amin, and O. A. Mohammed, "Robust Adaptive Neural Network Tracking Control With Optimized Super-Twisting Sliding-Mode Technique for Induction Motor Drive System," IEEE Transactions on Industry Applications, vol. 58, no. 3, pp. 4134–4157, May 2022, doi: 10.1109/TIA.2022.3160136.

[10] D. Cherifi and Y. Miloud, "Hybrid Control Using Adaptive Fuzzy Sliding Mode Control of Doubly Fed Induction Generator for Wind Energy Conversion System," Periodica Polytechnica Electrical Engineering and Computer Science, vol. 64, no. 4, Art. no. 4, Sep. 2020, doi: 10.3311/PPee.15508.

[11] A. Benhammou, M. A. Hartani, H. Tedjini, H. Rezk, and M. Al-Dhaifallah, "Improvement of Autonomy, Efficiency, and Stress of

Fuel Cell Hybrid Electric Vehicle System Using Robust Controller," Sustainability, vol. 15, no. 7, Jan. 2023, doi: 10.3390/su15075657.

[12] J. Guo, K. Li, J. Fan, Y. Luo, and J. Wang, "Neural-Fuzzy-Based Adaptive Sliding Mode Automatic Steering Control of Vision-based Unmanned Electric Vehicles," Chinese Journal of Mechanical Engineering, vol. 34, no. 1, p. 88, Sep. 2021, doi: 10.1186/s10033-021-00597-w.

[13] Guo Qing Geng, Peng Cheng, Li Qin Sun, Xing Xu, and Fanqi Shen, "A Study on Lateral Stability Control of Distributed Drive Electric Vehicle Based on Fuzzy Adaptive Sliding Mode Control," International Journal of Automotive Technology, vol. 25, no. 6, pp. 1415–1429.

[14] B. Mohammed, F. Bounaama, S. Bennaceur, B. Aissa, and M. Soumeur, "A Particle Swarm Optimization Based Fuzzy Flcpi-Pso Controller for Quadcopter System," Communications - Scientific letters of the University of Zilina, vol. 26, issue 3, Apr. 2024, doi: 10.26552/com.C.2024.027.

[15] T. Huang, X. Gao, and T. Li, "Adaptive Fuzzy Attitude Sliding Mode Control for a Quadrotor Unmanned Aerial Vehicle," Int. J. Fuzzy Syst., vol. 26, no. 2, Mar. 2024, pp. 686–701, doi: 10.1007/s40815-023-01628-5.

[16] Q. Shi, M. Wang, Z. He, C. Yao, Y. Wei, and L. He, "A Fuzzy-based Sliding Mode Control Approach for Acceleration Slip Regulation of Battery Electric Vehicle," Chinese Journal of Mechanical Engineering, vol. 35, no. 72, Jun. 2022, doi: 10.1186/s10033-022-00729-w.

[17] T. A. Nguyen, "A novel approach with a fuzzy sliding mode proportional integral control algorithm tuned by fuzzy method (FSMPIF)," Sci Rep, vol. 13,. 7327, May 2023, doi: 10.1038/s41598-023-34455-7.

[18] A. Haddoun, M. E. H. Benbouzid, D. Diallo, R. Abdessemed, J. Ghouili, and K. Srairi, "Modeling, analysis, and neural network control of an EV electrical differential," IEEE Transactions on industrial electronics, vol. 55, no. 6, pp. 2286–2294, 2008.

[19] L. Baghli, "Contribution to Induction Machine Control: Using Fuzzy Logic, Neural Networks and Genetic Algorithms," Henri Poincare University, Phd Thesis, 1999.

[20] V. I. Utkin, "Sliding mode control design principles and applications to electric drives," IEEE transactions on industrial electronics, vol. 40, no. 1, pp. 23–36, 2002.

[21] M. A. Hartani, A. Benhammou, and A. Laidi, "Performance Evaluation of PI and ST-SMC Controllers in Low Voltage/Power DC-Microgrids,", chapter in book: "Advances in Robust Control and Applications" edited by Mahmut Reyhanoglu, intechopen, 2025. DOI: 10.5772/intechopen.1006834

[22] R.-J. Wai, "Adaptive sliding-mode control for induction servomotor drive," IEE Proceedings-Electric Power Applications, vol. 147, no. 6, pp. 553–562, 2000.

[23] K. Makhloufi, I. K. Bousserhane, and S. A. Zegnoun, "Adaptive fuzzy sliding mode controller design for PMLSM position control," International Journal of Power Electronics and Drive Systems (IJPEDS), vol. 12, no. 2, Jun. 2021, pp. 674-684. doi: 10.11591/ijpeds.v12.i2.pp674-684.

[24] Q. Nguyen-Vinh and T. Pham-Tran-Bich, "Sliding mode control of induction motor with fuzzy logic observer," Electrical Engineering, vol. 105, no. 5, pp. 2769–2780, 2023.

[25] A. Nurettin and N. İnanç, "Design of a robust hybrid fuzzy super-twisting speed controller for induction motor vector control systems," Neural Comput & Applic, vol. 34, no. 22, pp. 19863–19876, Nov. 2022, doi: 10.1007/s00521-022-07519-4.

A. Ghezouani, G. Brahim, N. Nouria, O. Abdelkhalek, and J. Ghouili, "Comparative Study of PI and Fuzzy Logic Based Speed Controllers of an EV with Four In-Wheel Induction Motors Drive," Journal of Automation, Mobile Robotics and Intelligent Systems, vol. 12, N°. 3, Dec. 2018, pp. 43–54. doi: 10.14313/JAMRIS_3-2018/17.